Supplemental File of Data-driven Linear-Time-Variant MPC Method for Voltage and Power Regulation in Active Distribution Networks

Siyun Li, Wenchuan Wu, *Fellow, IEEE*

I. Convergence Analysis of the Proposed Data-driven LTV-MPC Algorithm

At every time instant, the optimization problem to be solved can be written compactly as the following nonlinear program (NLP):

$$\begin{aligned} \min_{w} \quad & \phi(w) \\ s.t. \quad & g(w,\mu)=0 \\ & h(w)\le 0 \end{aligned} \tag{1}$$

where $w=(u,x)\in R^{p}$ are the decision variables, u is the control sequence, and x is the state sequence. μ is the parameter, such as the predictions of load and PV at every time instant. The Lagrangian associated with (1) is

$$L(w,\lambda,v,\mu)=\phi(w)+\lambda^{T}g(w,\mu)+v^{T}h(w) \tag{2}$$

where λ and v are dual variables. Its KKT conditions can be written as [1]

$$\begin{aligned} &\nabla_{w}L(w,\lambda,v,\mu)=0 \\ &-g(w,\mu)=0 \\ &-h(w)+\mathcal{N}_{+}(v)\ni 0 \end{aligned} \tag{3}$$

where $\mathcal{N}_{+}$ is the normal cone mapping of the non-negative orthant. (See [2] for more background on set-valued and normal cone mappings.)

Define $z=(w,\lambda,v)$, and

$$F(z,\mu)=\begin{bmatrix} \nabla_{w}L(w,\lambda,v,\mu) \\ -g(w,\mu) \\ -h(w) \end{bmatrix} \tag{4}$$

Then KKT conditions (3) can be written as a parameterized generalized equation of the form

$$F(z,\mu)+\mathcal{N}_{K}(z)\ni 0 \tag{5}$$

where $\mathcal{N}_{K}$ is the normal cone mapping of a closed, convex set K [2].

The solution mapping of (5) is

$$S^{*}(\mu)=\{z\mid F(z,\mu)+\mathcal{N}_{K}(z)\ni 0\} \tag{6}$$

The domain of the solution mapping is the set of feasible parameters, i.e., $\operatorname{dom} S=\Gamma$.

To solve the NLP (1), the sequential quadratic programming (SQP) scheme is stated as follows. Given a solution estimate z_i, the next iterate z_{i+1} can be computed by solving the following quadratic program (QP)

$$\begin{aligned} \min_{\Delta w_i} \quad & \frac{1}{2}\Delta w_i^{T}B_i\Delta w_i+\nabla_{w}\phi(z_i)^{T}\Delta w_i \\ s.t. \quad & \nabla_{w}g(w_i,x)\Delta w_i+g(w_i,\mu)=0 \\ & \nabla_{w}h(w_i)\Delta w_i+h(w_i)\le 0 \end{aligned} \tag{7}$$

where B_i approximates the Hessian of the Lagrangian $\nabla_{w}^{2}L$. If we denote the Lagrange multipliers associated with the equality and the inequality constraints by π_i and η_i, with $\Delta w_i=w-w_i$, the SQP update for the NLP (1) is $z_{i+1}=(w_i+\Delta w_i,\pi_i,\eta_i)$.

Note that B_i will depend on the specific SQP method. When ϕ is convex, $B_i=\nabla_{w}^{2}\phi(w_i)$ is a sufficiently good approximation [3]. In our problem formulation, ϕ is a convex quadratic function, so we apply the approximation $B_i=\nabla_{w}^{2}\phi(w_i)$. Note that in this case, the objective function in (7) is equivalent to the original objective function ϕ, so the problem (7) can be written as

$$\begin{aligned} \min_{w} \quad & \phi(w) \\ s.t. \quad & \nabla_{w}g(w_i,x)(w-w_i)+g(w_i,\mu)=0 \\ & \nabla_{w}h(w_i)(w-w_i)+h(w_i)\le 0 \end{aligned} \tag{8}$$

To provide a unified formulation, we exploit that SQP can be seen as a Newton-type process for solving Generalized equations (5). Newton's method applied to (5) is

$$H_i(z_{i+1}-z_i)+F(z_i,\mu)+\mathcal{N}_{K}(z_{i+1})\ni 0 \tag{9}$$

where the sequence $\{H_i\}$ approximates $\nabla_{z}F(z_i,\mu)$.

Referring to the QP subproblem (7), we note that

$$H_i=\begin{bmatrix} B_i & \nabla_{w}^{T}g(w_i) & \nabla_{w}^{T}h(w_i) \\ -\nabla_{w}g(w_i) & 0 & 0 \\ -\nabla_{w}h(w_i) & 0 & 0 \end{bmatrix} \tag{10}$$

The proposed data-driven method can be seen as a variant of SQP. The difference is, the proposed method use a data-driven method to approximate the linearization around the previous solution estimate without knowledge of the system parameters, while the original SQP uses the derivative of functions to provide the linearization around the previous solution estimate relying on the exact system model.

Therefore, similar to (9), the update for the proposed data-driven method can be written as

$$\hat{H}_i(z_{i+1}-z_i)+\hat{F}(z_i,\mu)+\mathcal{N}_K(z_{i+1})\ni 0 \tag{11}$$

$$\hat{H}_i=\begin{bmatrix} B_i & A_g(w_i) & A_h(w_i) \\ -A_g(w_i) & 0 & 0 \\ -A_h(w_i) & 0 & 0 \end{bmatrix} \tag{12}$$

$$\hat{F}(z_i,\mu)=\begin{bmatrix} \nabla_w \hat{L}(w_i,\lambda_i,v_i,\mu) \\ -\hat{g}(w_i,\mu) \\ -\hat{h}(w_i) \end{bmatrix} \tag{13}$$

where $A_g(w_i)$ and $A_h(w_i)$ are parameter matrix obtained based on our data-driven linearization, which correspond to the estimation of $\nabla_w g(w_i)$ and $\nabla_w h(w_i)$ respectively. $\nabla_w \hat{L}(w_i,\lambda_i,v_i,\mu)$, $\hat{g}(w_i,\mu)$ and $\hat{h}(w_i)$ are the estimation of functions based on our data-driven approximation, corresponding to $\nabla_w L(w_i,\lambda_i,v_i,\mu)$, $g(w_i,\mu)$ and $h(w_i)$ respectively.

If the data-driven power flow approximation is sufficiently accurate, it is reasonable to have the following assumptions.

Assumption 1. For some fixed parameter $\mu\in\Gamma$, and the optimal solution $z^*\in S^*(\mu)$, there exists $\overline{\delta}=\overline{\delta}(\mu)>0$ such that $\left\|\hat{H}_i-\nabla F(z^*,\mu)\right\|\le\overline{\delta}$ for all $i\ge 0$.

Assumption 2. For any z' and z'', the error between the estimated value $\hat{F}(z')-\hat{F}(z'')$ and real value $F(z')-F(z'')$ is bounded as

$$\begin{aligned}&\left\|\left(\hat{F}(z')-\hat{F}(z'')\right)-\left(F(z')-F(z'')\right)\right\| \\ &\le\theta_s\left\|F(z')-F(z'')\right\|\end{aligned} \tag{14}$$

where θ_s is a small enough non-negative scalar.

The convergence analysis for the proposed method is similar to [3]. The following theorem establishes sufficient conditions for q-linear convergence of the proposed data-driven method by extending the classical fixed-point type analysis of Newton's method [4].

Theorem 1. For some fixed parameter $\mu\in\Gamma$, let $z^*\in S^*(\mu)$ and suppose that **Assumption 1** and **Assumption 2** hold. Consider a sequence $\{z_i\}$ generated by repeatedly solving (11). Further, define $e_i=z_i-z^*$ and suppose that function F and ∇F is Lipschitz continuous. If the mapping $J_i(z)=\hat{H}_i z+\mathcal{N}_K(z)$ is strongly regular for all $i\ge 0$, i.e., J_i^{-1} is a Lipschitz continuous function with Lipschitz constant $M>0$, and $M(\overline{\delta}+\theta_s L)<1$, where L is the Lipschitz constant of function F, then there exists $\overline{\epsilon}=\epsilon(\mu)>0$, such that if $z_0\in\overline{\epsilon}\mathcal{B}(z^*)$, then $\{z_i\}$ converges to z^* q-linearly, and

$$\|e_{i+1}\|\le\overline{\eta}\|e_i\|,\quad\forall e_i\in\overline{\epsilon}\mathcal{B} \tag{15}$$

where $\overline{\eta}=M(\overline{\delta}+\theta_s L+L\overline{\epsilon}/2)<1$.

Proof. An optimal solution $z^*\in S^*(\mu)$ exists for every $\mu\in\Gamma$, since Γ is the set of feasible parameters. From this point forward we will suppress the dependencies on μ in the subsequent expressions. The proposed data-driven update method can be written as

$$z_{i+1}=J_i^{-1}\circ G_i(z_i)=T_i(z_i) \tag{16}$$

where $G_i(z)=\hat{H}_i z-\hat{F}(z)$, $J_i(z)=\hat{H}_i z+\mathcal{N}_K(z)$; note that $z^*=T_i(z^*)$ for any choice of $\{\hat{H}_i\}$. First consider

$$\begin{aligned}&G_i(z_i)-G_i(z^*)=\hat{H}_i(z_i-z^*)-\hat{F}(z_i)+\hat{F}(z^*) \\ &=\nabla F(z^*)(z_i-z^*)-F(z_i)+F(z^*) \\ &+(\hat{H}_i-\nabla F(z^*))(z_i-z^*) \\ &+\hat{F}(z^*)-\hat{F}(z_i)-(F(z^*)-F(z_i))\end{aligned} \tag{17}$$

We denote the unit ball centered at z^* by $\mathcal{B}(z^*)$. It is assumed that F and ∇F is Lipschitz continuous, the fundamental theorem of calculus implies that there exist L, $\epsilon_1>0$ such that

$$\left\|F(z_i)-F(z^*)\right\|\le L\left\|z_i-z^*\right\| \tag{18}$$

$$\left\|\nabla F(z^*)(z_i-z^*)-F(z_i)+F(z^*)\right\|\le\frac{L}{2}\left\|z_i-z^*\right\|^2 \tag{19}$$

for all $z_i\in\epsilon_1\mathcal{B}(z^*)$.

Combine (18) and (14), we have

$$\begin{aligned}&\left\|\left(\hat{F}(z_i)-\hat{F}(z^*)\right)-\left(F(z_i)-F(z^*)\right)\right\| \\ &\le\theta_s\left\|F(z_i)-F(z^*)\right\| \\ &\le\theta_s L\left\|z_i-z^*\right\|\end{aligned} \tag{20}$$

Therefore, taking norms in (17), we obtain that

$$\left\|G_i(z_i)+G_i(z^*)\right\|\le\frac{L}{2}\left\|z_i-z^*\right\|^2+(\overline{\delta}+\theta_s L)\left\|z_i-z^*\right\| \tag{21}$$

By assumption, the mapping J_i^{-1} is Lipschitz continuous so $\Delta T_i^*=\left\|T_i(z)-T_i(z^*)\right\|$ satisfies

$$\begin{aligned}\Delta T_i^*&=\left\|J_i^{-1}(G_i(z_i))-J_i^{-1}(G_i(z^*))\right\| \\ &\le M\left\|G_i(z_i)-G_i(z^*)\right\| \\ &\le M(\overline{\delta}+\theta_s L+\frac{L}{2}\|e_i\|)\|e_i\|\end{aligned} \tag{22}$$

For all $z_i\in\epsilon_1\mathcal{B}(z^*)$. Now consider the update equation

$$\left\|z_{i+1}-z^*\right\|=\left\|T_i(z_i)-z^*\right\|=\left\|T_i(z_i)-T_i(z^*)\right\| \tag{23}$$

where we have used that $z^*=T_i(z^*)$. Since J_i is strongly regular, T_i is a function and $\{z_i\}$ is unique. Using (22) we have

$$\|e_{i+1}\|\le M(\overline{\delta}+\theta_s L+L\|e_i\|/2)\|e_i\|,\quad\forall e_i\in\epsilon_1\mathcal{B} \tag{24}$$

Since $M(\bar{\delta}+\theta_s L)<1$ by assumption, it is possible to pick $\bar{\epsilon}\in(0,\epsilon_1)$ such that $\bar{\eta}=M(\bar{\delta}+\theta_s L+L\bar{\epsilon}/2)<1$. Then $\{z_i\}$ converges q-linearly to z^* if $z_0\in\bar{\epsilon}\mathcal{B}(z^*)$, i.e.,

$$\|e_{i+1}\|\le\bar{\eta}\|e_i\|,\quad \forall e_i\in\bar{\epsilon}\mathcal{B} \tag{25}$$

■

Now we have provided the convergence analysis for the proposed data-driven method if the fully converged solution is obtained by iterations at every sampling instant.

Next, we consider the application of time-distributed optimization in a real-time setting, where it is only possible to perform a finite number of iterations per sampling instant which we denote by $\ell\in\mathbb{Z}_{++}$. The Algorithm 2 provided in the paper is the spatial case with $\ell=1$.

In our MPC scheme, the control actions are obtained through solving an H-horizon optimization problem at each time instant. However, only the current (or the first) time-step control move is implemented and at the next sampling time, the optimization problem is reformulated.

Therefore, in the following, we now turn to analyze the optimality of the current (or the first) time-step control move calculated at time t. Suppose that $t\ge H$ and $H>2$. From this point forward we denote the control actions that should be implemented at time $t+1$ as $u(t+1)$. For $t-H+1\le v\le t$, $u_v(t+1)$ refers to the calculation result of the action should be implemented at time $t+1$ which is calculated at time v. Note that only $u_t(t+1)$ obtained at time t is implemented to the system.

Assumption 3. For $t-H+1\le v\le t$, variation of the optimal solution of the H-horizon optimization problem at each sampling instant is bounded as

$$\|u_v^*(t+1)-u_{v-1}^*(t+1)\|\le\theta_C \tag{26}$$

where $u_v^*(t+1)$ and $u_{v-1}^*(t+1)$ refer to the optimal solution of the action that should be implemented at time $t+1$ in the H-horizon optimization problem formulated at time v and time $v-1$ respectively.

According to the q-linear convergence that we have proved, at time t, if the control result to be implemented next is calculated after ℓ iterations, denoted as $u_t^\ell(t+1)$, the following condition is satisfied for $u_t^0(t+1)\in\bar{\epsilon}\mathcal{B}\left(u_t^*(t+1)\right)$:

$$\|u_t^\ell(t+1)-u_t^*(t+1)\|\le(\bar{\eta})^\ell\|u_t^0(t+1)-u_t^*(t+1)\| \tag{27}$$

Similarly, the result for $u(t+1)$ calculated at time $t-1$ after ℓ iterations is $u_{t-1}^\ell(t+1)$, which satisfies

$$\|u_{t-1}^\ell(t+1)-u_{t-1}^*(t+1)\|\le(\bar{\eta})^\ell\|u_{t-1}^0(t+1)-u_{t-1}^*(t+1)\| \tag{28}$$

In the proposed scheme, the initial guess of the action $u_t^0(t+1)$ at time t equals the calculation result obtained at time $t-1$, i.e., $u_{t-1}^\ell(t+1)=u_t^0(t+1)$.

Thus, exploiting (28) and (26), we have

$$\begin{aligned}
&\|u_t^0(t+1)-u_t^*(t+1)\|\\
&=\|u_{t-1}^\ell(t+1)-u_{t-1}^*(t+1)+u_{t-1}^*(t+1)-u_t^*(t+1)\|\\
&\le\|u_{t-1}^\ell(t+1)-u_{t-1}^*(t+1)\|+\|u_{t-1}^*(t+1)-u_t^*(t+1)\|\\
&\le\bar{\eta}^\ell\|u_{t-1}^0(t+1)-u_{t-1}^*(t+1)\|+\|u_{t-1}^*(t+1)-u_t^*(t+1)\|\\
&\le\bar{\eta}^\ell\|u_{t-1}^0(t+1)-u_{t-1}^*(t+1)\|+\theta_C
\end{aligned} \tag{29}$$

Similarly, considering time $t-2$, we have

$$\begin{aligned}
&\|u_{t-1}^0(t+1)-u_{t-1}^*(t+1)\|\\
&\le\bar{\eta}^\ell\|u_{t-2}^0(t+1)-u_{t-2}^*(t+1)\|+\|u_{t-2}^*(t+1)-u_{t-1}^*(t+1)\|\\
&\le\bar{\eta}^\ell\|u_{t-2}^0(t+1)-u_{t-2}^*(t+1)\|+\theta_C
\end{aligned} \tag{30}$$

Therefore, similar to (29) and (30), by recurrence formula, we have

$$\begin{aligned}
&\|u_t^0(t+1)-u_t^*(t+1)\|\\
&\le\bar{\eta}^{(H-1)\ell}\|u_{t-H+1}^0(t+1)-u_{t-H+1}^*(t+1)\|+\\
&[1+\bar{\eta}^\ell+\bar{\eta}^{2\ell}+\ldots+\bar{\eta}^{(H-2)\ell}]\theta_C\\
&\le\bar{\eta}^{(H-1)\ell}\|u_{t-H+1}^0(t+1)-u_{t-H+1}^*(t+1)\|+\frac{1-\bar{\eta}^{(H-1)\ell}}{1-\bar{\eta}^\ell}\theta_C
\end{aligned} \tag{31}$$

Note that the optimization problem at each time instant is an H-horizon one, so at time $t-H+1$, $u_{t-H+1}^\ell(t+1)$ is the last element of the calculated predictive control sequence.

Combing (31) and (27), we have

$$\begin{aligned}
&\|u_t^\ell(t+1)-u_t^*(t+1)\|\le(\bar{\eta})^\ell\|u_t^0(t+1)-u_t^*(t+1)\|\\
&\le\bar{\eta}^{H\ell}\|u_{t-H+1}^0(t+1)-u_{t-H+1}^*(t+1)\|+\bar{\eta}^\ell\frac{1-\bar{\eta}^{(H-1)\ell}}{1-\bar{\eta}^\ell}\theta_C
\end{aligned} \tag{32}$$

According to (32), for $t\ge H$ and $H>2$, if the initial guess at $t-H+1$, i.e., $u_{t-H+1}^0(t+1)$, is close enough to the optimal one, i.e., $u_{t-H+1}^*(t+1)$, and the system variation bound θ_C is limited, then the control action finally implemented to the system $u_t^\ell(t+1)$ can approximate the optimal solution $u_t^*(t+1)$ sufficiently.

II. TEST SYSTEMS

The figure of cases are illustrated in figs. 1 and 2. The normalized curves of total output of PVs and load demand are illustrated in Fig. 3.

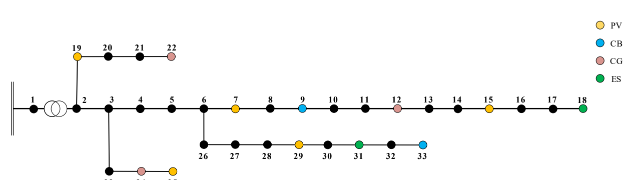

Fig. 1. Modified 33-bus system

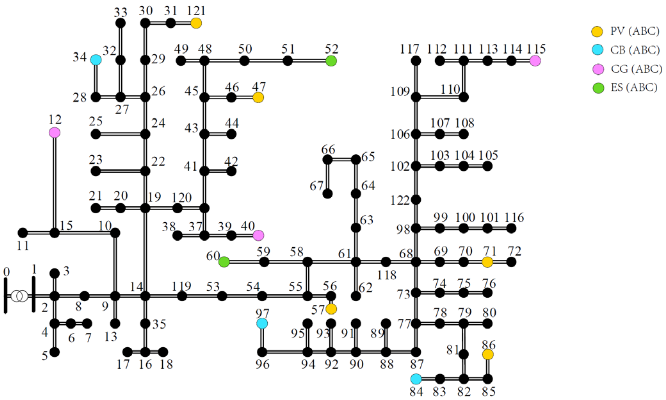

Fig. 2. Modified three-phase unbalanced 123-bus system

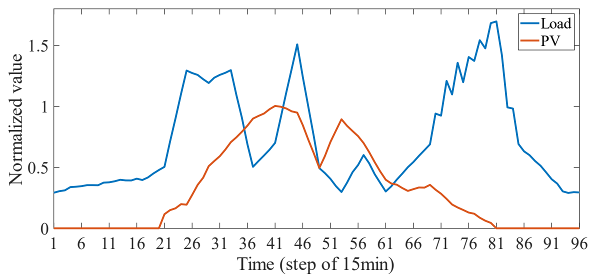

Fig. 3. Load and PV profiles

III. HYPERPARAMETERS

The algorithm hyperparameters are shown in Table I. The size of the training dataset for the 33-bus case and 123-bus case are 10000 and 20000 respectively.

In the PWL-SVR algorithm, the regression parameters $\{\boldsymbol{w}_k^0, \boldsymbol{b}_k^0\}_{k=1}^K$ and $S_1^0,\ldots,S_K^0$ are initialized as follows: the data $\boldsymbol{x}_n$, $n=1,\ldots,N$ is clustered into K clusters using K-means clustering. This gives us the initial cluster set $S_1^0,\ldots,S_K^0$. Then in each cluster we do the linear SVR regression, and this gives us initial regression parameters $\{\boldsymbol{w}_k^0, \boldsymbol{b}_k^0\}_{k=1}^K$.

The objective parameters in the MPC formulation are shown in Table II. If the parameters are different in the 33-bus and 123-bus cases, they would be listed in $\{\cdot,\cdot\}$.

TABLE I
ALGORITHM HYPERPARAMETERS

Algorithm	Parameter	value
PWL-SVR regression	K	{30,50}
	C	$\{10^3\}$
	σ	$\{10^{-2}\}$
	ϵ	{0.005}
	β	$\{10^{-3}\}$
	$c_{\max}$	{50}

TABLE II
OBJECTIVE PARAMETERS

Item	value	Item	value	Item	value
c_{ele}	{2.5, 3.5}	λ_{OLTC}	{6}	λ_{PV}	{500, 200}
λ_{CB}	{1.8, 2}	λ_x	{3000, 400}	a_1	{0.05}
a_2	{0.06}	a_3	{0.08}	b_1	{3}
b_2	{4}	b_3	{5}		

IV. DETERMINATION OF THE CLUSTER NUMBER

We test the accuracy of our method with different K values. Fig. 4 illustrates the mean absolute percentage error of the voltage magnitudes of the 33-bus system. We observe that the regression error decreases with the K value increases. However, the accuracy improves slowly after K increases to a certain large value.

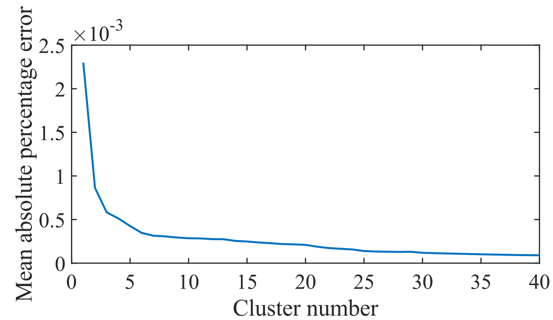

Fig. 4. Mean absolute percentage error of the voltage magnitudes of the 33-bus system.

V. DISCUSSION OF THE PREDICTION ERROR

In practice, the predicted values are different from the actual values. To better match the real situation, simulations are performed on the 33-bus case with the consideration of prediction error. According to [5], we assume that the real-time prediction error follows normal distribution with zero mean and the standard deviation of 5%. To validate the effectiveness of the proposed method under prediction error, the model-based optimal results using the actual values as the predicted values are adopted as a benchmark.

TABLE III
COMPARISON OF RELATIVE ERRORS IN ACCUMULATED COST

	Accumulated cost	Accumulated cost error
Model-based	2686.19	-
Proposed	2732.26	6.51%
LTI	3434.42	27.85%

The accumulated cost function value at every time step and the control results under prediction error are shown in Fig. 5. and Fig. 6, respectively. It can be seen that the proposed method has achieved similar performance to the model-based optimal solver with an accurate system model. To validate the accuracy, Table III shows the relative errors between the data-driven control results under prediction error and the accurate model-based optimal results in accumulated cost function value at the end of the day.

We can see that the proposed method can still provide sufficiently good results under a certain range of prediction error. However, to better consider the prediction error, expanding the proposed method to combine other stochastic optimization techniques such as robust optimization to further consider the prediction uncertainty is an interesting topic for future work. We look forward to exploring this topic in our future research.

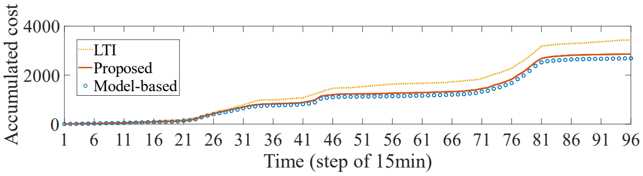

Fig. 5. Accumulated cost in 33-bus test case.

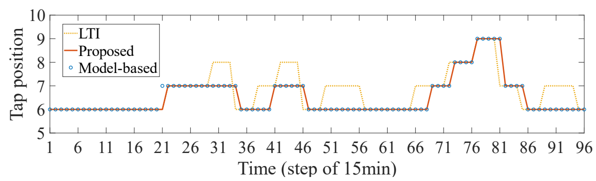

(a) Control results of the OLTC.

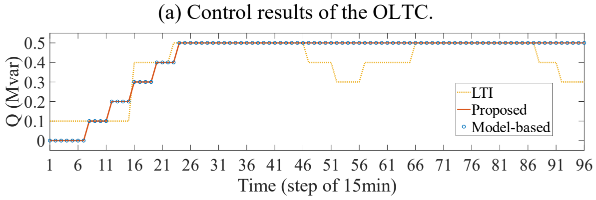

(b) Reactive power output of CB 1.

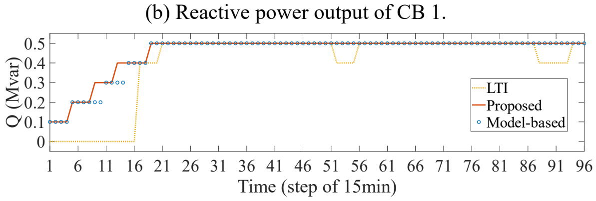

(c) Reactive power output of CB 2.

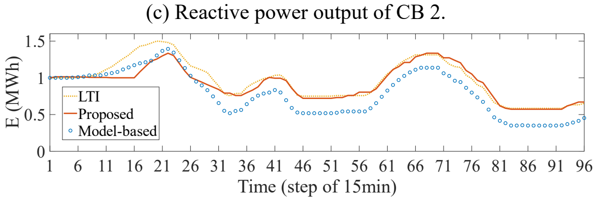

(d) Total energy stored in ESs.

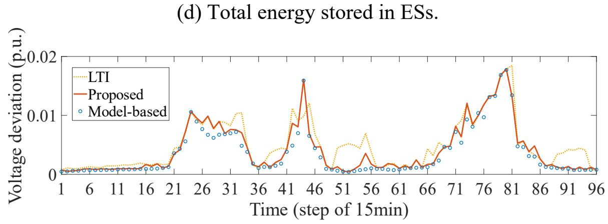

(e) Mean absolute deviation of voltage magnitude.

Fig. 6. Control results in 33-bus test case with prediction error.

VI. Numerical Tests on the System with Loops

The proposed data-driven method is not limited to radial network topology. To demonstrate that the proposed method can also be applied to looped distribution systems, we have tested the method on a modified 33-bus system with loops. The topology of the tested system is shown in Fig. 7.

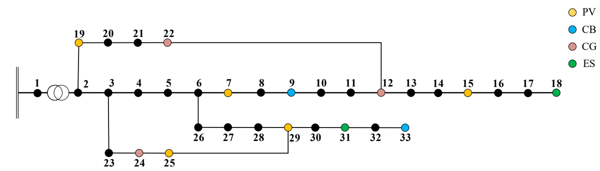

Fig. 7. Modified 33-bus system with loops.

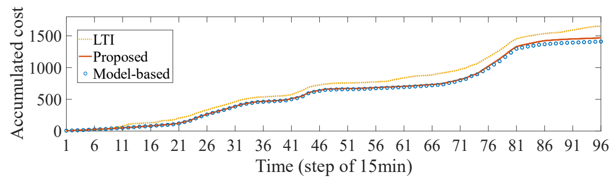

Fig. 8. Accumulated cost in 33-bus system with loops.

The accumulated cost function value at every time step is shown in Fig.8. It can be seen that the proposed method has achieved similar performance to the model-based optimal solver with an accurate system model. Fig.9 details the control results of the compared control strategies. Specifically, the relative errors between several control results and the accurate model-based optimal results in accumulated cost function value at the end of the day are shown in Table IV.

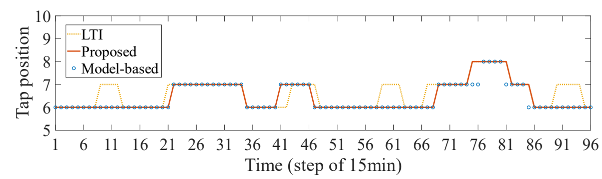

(a) Control results of the OLTC.

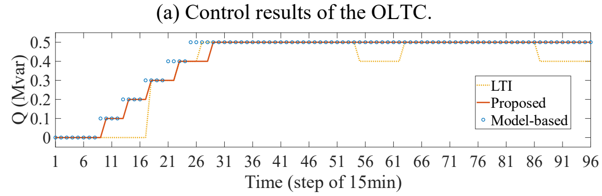

(b) Reactive power output of CB 1.

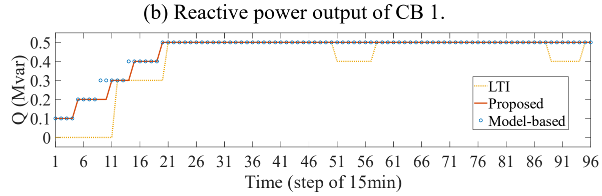

(c) Reactive power output of CB 2.

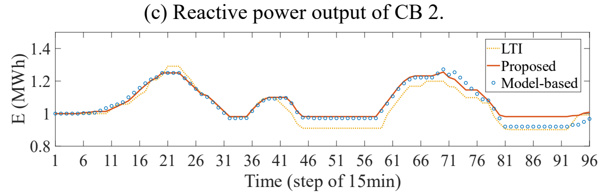

(d) Total energy stored in ESs.

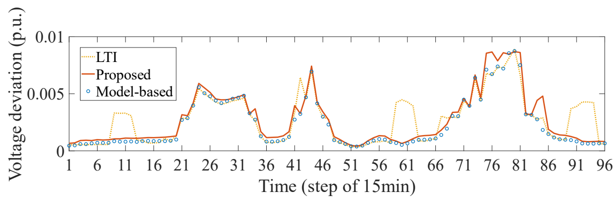

(e) Mean absolute deviation of voltage magnitude.

Fig. 9. Control results in modified 33-bus system with loops.

TABLE IV

COMPARISON OF RELATIVE ERRORS IN ACCUMULATED COST

	Accumulated cost	Accumulated cost error
Model-based	1410.31	-
Proposed	1464.71	3.85%
LTI	1651.46	17.10%

References

[1] A. F. Izmailov and M. V. Solodov, *Newton-Type Methods for Optimization and Variational Problems*. in Springer Series in Operations Research and Financial Engineering. Cham: Springer International Publishing, 2014. doi: 10.1007/978-3-319-04247-3.

[2] A. L. Dontchev and R. T. Rockafellar, *Implicit Functions and Solution Mappings*. in Springer Series in Operations Research and Financial Engineering. New York, NY: Springer, 2014. doi: 10.1007/978-1-4939-1037-3.

[3] D. Liao-McPherson, M. M. Nicotra, and I. Kolmanovsky, "Time-distributed optimization for real-time model predictive control: Stability, robustness, and constraint satisfaction," *Automatica*, vol. 117, p. 108973, Jul. 2020, doi: 10.1016/j.automatica.2020.108973.

[4] C. T. Kelley, *Iterative methods for linear and nonlinear equations*. SIAM, 1995.

[5] Y. Du, W. Pei, N. Chen, X. Ge, and H. Xiao, "Real-time microgrid economic dispatch based on model predictive control strategy," *J. Mod. Power Syst. Clean Energy*, vol. 5, no. 5, pp. 787–796, Sep. 2017, doi: 10.1007/s40565-017-0265-4.